OPEN ACCESS
Freely Available Online

INTERNATIONAL JOURNAL OF LIPIDS
ISSN NO: 2835-513X

Special Issue
DOI: 10.14302/issn.2835-513X.ijl-20-3454

Insights on the Thermal and Physical Stability of the Modified Polymerizable Liposomes for Improved Photoactivity

Poornima Kalyanram[1], Noor Hussein[2], Amit Tiwari[2], Anju Gupta[3,*]

[1]College of Engineering, Rochester Institute of Technology, Rochester, NY 14623, USA

[2]Department of Pharmacology and Experimental Therapeutics, University of Toledo, Toledo, OH 43614, USA

[3]Department of Mechanical, Industrial and Manufacturing Engineering, University of Toledo, Toledo, OH 43614, USA

Abstract

We investigated physical steric and thermal stability effects induced by cholesterol and polyethylene glycol (PEG) in liposomes encapsulated with riboflavin. The composition of liposome was varied systematically to decipher the individual and combined effects of cholesterol and PEG on the stabilization of liposomes, specially the photopolymerizable liposomes for their potential applications in photo-treatments. Our results indicate that inclusion of PEG in the lipids enhances the steric stabilization by adopting a brush-like regime that prevents the agglomeration of encapsulated liposomes. A mechanistic differential scanning calorimetry studies reveal the phase transitions and enthalpy changes in the lipid bilayer due to the presence of cholesterol suggesting its role in regulating membrane fluidity. Supporting *in- vitro* studies confirm the efficacy of PEGylated formulations encapsulating riboflavin.

Corresponding author: Anju Gupta, Department of Mechanical, Industrial and Manufacturing Engineering, University of Toledo, Toledo, OH 43614, USA, Phone: +1 419- 530- 8213 Email: anju.gupta@utoledo.ed

Keywords: Drug carriers, Thermal analysis, Polymer, Lipid bilayer, Steric stabilization, Cholesterol

Received: Jul 23, 2020 **Accepted:** Aug 08, 2020 **Published:** Sep 08, 2020

Editor: Abdelkarim ABOUSALHAM, UniversitÃ© de Lyon; UNIVERSITE CLAUDE BERNARD LYON 1, CNRS, INSA-LYON, CPE-LYON 43, Bd du 11 novembre 1918 69622 Villeurbanne cedex FRANCE

Introduction

Liposomes or phospholipid vesicles offer several advantages in theragnostic due to their biocompatibility [1, 2], ease of surface functionalization [3, 4], and their ability to entrap both hydrophilic [5, 6] and hydrophobic drugs and targets [7, 8]. However, the stability and leakiness of the phospholipid-based vesicles pose limitations for their applications in targeted delivery that require longer circulation periods in human bodies [9, 10]. Several strategies such as inclusion of cholesterol, photopolymerizable lipids, polymeric lipids through conjugation of polyethylene glycol (PEG) have been exploited to overcome the poor stability of the liposomes [11–13]. Photopolymerizable lipids consist of conjugated diynes in their alkyl tails, that can be stimulated by UV (ultra-violet) light [14, 15], this aids in prevention of leakage and sustained release of contents[16–18].

The PEG molecules are known to cause steric stabilization in the liposomes. The hydrophilic PEG chains cover the surface of the lipid bilayer and extend and stay associated with the aqueous bulk instead of interacting with other molecules on the nearby liposomes [19, 20]. Additionally, as the concentration of the PEG molecules increases in the bulk, the water molecules balance out by diluting the bulk concentration of PEG by keeping the PEG molecules apart, thereby preventing the agglomeration of PEGylated liposomes [20–22]. In addition to PEG, cholesterol is also used in liposomal formulations to induce rigidity to the bilayer to further control the inherent leakiness of the liposomes [23, 24]. Cholesterol is also known to regulate the fluidity, permeability and packing of the bilayer [25, 26]. Both cholesterol and PEG enriched liposomes have been approved by FDA for delivery of the potent drugs including doxorubicin as (Doxil®) and irinotecan (Onivyde™) [27]. However, cholesterol has shown to undergo oxidization in the presence of reactive oxygen species (ROS) resulting in the production of cholesterol oxidation products (COPs) or derivatives of oxysterols such as 7- ketocholesterol, 20α-hydroxycholesterol, 25-hydroxycholesterol, α,β-epoxycholesterol, and 7α, 7β-hydroxycholesterol, that cause atherogensis in humans [23, 28–33]. Additionally, the majority of the cholesterol used in commercially available and FDA approved liposomal formulations in drug delivery and vaccine are derived from animal sources such as egg or wool grease that poses a threat of contamination and allergies [34].

In this work, we have investigated the stability of a Riboflavin encapsulated liposomes comprising of photopolymerizable lipid $DC_{8,9}PC$ lipids along with DSPE-PEG2000 and cholesterol. Riboflavin was used as a model photosensitizer to test the efficacy of liposomal formulations in vitro for potential applications in Photo Dynamic Therapy (PDT) [35–37]. The work primarily focused on: thermal stability of the liposomal formulations through phase transition thermodynamics studies using Differential Scanning Calorimetry (DSC) assessing the contributions of PEG and cholesterol in the physical stability of liposomal formulation

Our findings indicate that the thermal and physical stability of the liposomal formulations can be achieved by exploiting the PEG ratio, and the choice of the lipid, thereby, eliminating the need of cholesterol. Such cholesterol-limiting liposomal formulations can address the safety concerns associated with the use of animal-derived cholesterol and further investigations are warranted to determine the optimum lipid type and PEG ratio for enhanced stability for the liposomes.

Materials and Methods

Materials

23:2 Diyne PC [$DC_{8,9}PC$] (1,2-bis(10,12-tricosadiynoyl)-sn-glycero-3-phosphocholine) and DSPE-PEG-2000(1,2-distearoyl-sn-glycero-3-phosphoethanolamine - N[methoxy(polyethyleneglycol)-2000] (ammonium salt)) suspended in chloroform were purchased from Avanti Polar Lipids (Alabaster, AL). Cholesterol and Riboflavin-5-phosphate sodium salt dihydrate were procured from Sigma Aldrich. Invitrogen™ RNase-free PBS - Phosphate-Buffered Saline (PBS) pH 7.4 was purchased from Fisher Scientific. Invitrogen™ e-Bioscience™ Annexin V Apoptosis Detection Kit PE and 7-amino-actinomycin D (7-AAD) components were purchased from Fisher Scientific.

Preparation of Liposomes

Lipids and cholesterol were suspended in chloroform. The lipid mixtures were dried under ultra-pure nitrogen environment to obtain a thin film in the bottom of the tubes that were hydrated with PBS buffer (10X) of pH 7.4. For the encapsulated liposomes, riboflavin was suspended the PBS buffer prior to

hydration of dried films. On re-hydration, liposomes were uniformly sized by extruding through polycarbonate membrane of pore size 100 nm. Liposomes were prepared using thin film hydration technique and sized as described in prior literature [38–42]. Details of the formulations are given in Table 1. The unencapsulated riboflavin was removed by ultracentrifugation followed by rinsing with fresh batch of PBS buffer. The total liposome to riboflavin ratio was maintained at 20:1 by weight ratio in this study.

Dynamic Light Scattering (DLS)

The size, polydispersity index (PDI) and surface charge of both encapsulated and unencapsulated liposomes were analyzed using a Malvern Instruments Zetasizer by dynamic light scattering method at 25 °C and at 173° backscatter angle with 120 s equilibration time.

Differential Scanning Calorimetry

10 µl of the liposome samples were placed in T-zero Hermetic pan. The pans were sealed with a sample press prior to placing them on a TA Instruments Q-2000 DSC. The DSC scans were performed in an inert nitrogen environment maintained at 40 mL/min in the temperature range of 25 to 65ºC at a heating rate of10 ºC/min. The stability study for these formulations was conducted using a Differential Scanning Calorimetry (DSC) for a four-week time frame. DSC measures the specific heat capacity as a function of temperature. In this case lipids, on heating undergo a gel to fluid crystalline endothermic transition. These transitions are detected by the DSC and the main transition is a sharp intense peak that occurs at the melting point. The nature of the transition is affected in the presence of other molecules[43, 44]. Any changes in the enthalpy of transition is measured from the area under the peak given by:

$$\text{Calorimetric Enthalpy: } \Delta H_C = \int C_p dT \quad \text{..(i)}$$

Where C_p is the heating capacity. The changes in enthalpy is an indicator of stability.

Apoptotic Studies

e-Bioscience™ Annexin V Apoptosis Detection PE and 7-AAD Kits for flow cytometry were used to measure early and late-stage apoptosis in human prostate cancer cells (DU- 145).Briefly, the cells were grown in cell culture media (DMEM) supplemented with 4.5 g of glucose, 10% fetal bovine serum (FBS) and 1% penicillin/streptomycin). The cells were grown in cell culture flasks to form adherent monolayers and were stored in a humidified incubator at 37 °C and 5% CO_2. The cells were washed with PBS, seeded at a density of 5000 cells/well in 24 well plates, and allowed to grow overnight. Next day, riboflavin encapsulated liposomes at 200 µl volume were added to the cells. The cells were incubated overnight to ensure uptake of the liposomes. After 24 hr, the cells were treated with UV-light to cause photo-polymerization of $DC_{8,9}PC$ lipids and subsequent activation of the riboflavin-encapsulated liposomes. The cells were then collected and washed with ice-cold phosphate buffered saline (PBS) followed by cells resuspension in 100 µl of 1X Annexin V binding buffer on an ice-cold bath. 5 µl of Annexin V was added

Table 1. Details of the formulations used in the study

$DC_{8,9}PC$ (L1) /DSPE-PEG-2000 (L2) / Cholesterol mole ratio (mol%)	Formulation Name	Riboflavin (RB) added at lipid: RB (20:1) w/w ratio
90/ 10	L1/L2 (90/10)	NO
80/ 20	L1/L2 (80/20)	NO
87.5/ 7.5/ 5	L1/L2 (90/10) + Chol (5)	NO
77.5/ 17.5/ 5	L1/L2 (80/20) + Chol (5)	NO
90/ 10/ 0	L1/L2 (90/10) + RB	YES
87.5/ 7.5/ 5	L1/L2 (87.5/7.5) + Chol (5) + RB	YES

to the 100 µl of cell suspension and incubated for 10-15 mins at room temperature. Next, the cells were washed with ice-cold PBS and resuspended in 200 µl of 1X binding buffer. Then, 5 µl of 7-AAD viability staining solution was added to the cell suspension. Finally, flow cytometry was used to detect the fluorescence of stained cells at excitation/emission maxima: Annexin V PE®: 499/521 nm; 7-AAD®: 535/617 nm with BD FACSAria IIu High-Speed Cell Sorter flow cytometer from BD Biosciences (Becton- Dickinson, San Jose, CA, USA).The data were viewed and analyzed using FlowJo v10.2 software from FlowJo LLC (Ashland, OR, USA).

Results

Characterization of Liposomal Formulation: Hydrodynamic Diameter and Surface Charge

The size and surface charge of the liposomal formulations were recorded for four weeks. It was observed that the measured zeta potential of the formulations were in the range of - 0.347±0.0075 mV or near neutral consistent to the zwitterionic nature of the DSPE lipids [45]. The near constant zeta potential also confirms the absence of un-associated and excess riboflavin in the liposomal solution. The average hydrodynamic diameters and polydispersity indices (PDI) of the formulations measured over a period of weeks are summarized in Fig 1. The size measurements studies conducted in Week 1 indicated that all the formulations were within the acceptable size range of 70-140±5 nm at a PDI of less than 0.25±0.0005 mV indicating the uniformity of the extruded liposomes. However, after week 4, most of the formulations agglomerated with a significant increase in the measured average diameters. The presence of cholesterol did not affect the size or PDI of the formulations. It is also observed that with an increase in DSPE-PEG 2000 by 10 mol% the aggregation and dispersity of the particles also increased with time. It is implied that the presence of cholesterol has minimal influence on the physical stability of the liposomes with regards to the controlling the size and possibly their aggregation.

Differential Scanning Calorimetry-Thermal Stability Studies

In this work, we have focussed on the stability study through thermal characterization (DSC) technique. DSC was used to study the phase behaviour and changes in $DC_{8,9}PC$ and DSPE lipid in the presence of PEG and cholesterol. The resultant changes in the melting temperature and shape of the melting peak as summarized on Fig 2. The melting temperature represents the transition from gel to fluid phase of the lipid molecules represented on the x-axis, whereas the area under the melting peak corresponds to the calculated change in enthalpy, $\Delta H_C = \int C_p \, dT$ of the lipid formulations summarized on Table 2. C_p is the specific heat capacity of the lipids plotted on the y-axis. In a lipid bilayer, the fluidity and the movement of the lipid molecules constitute the internal energy of the system.

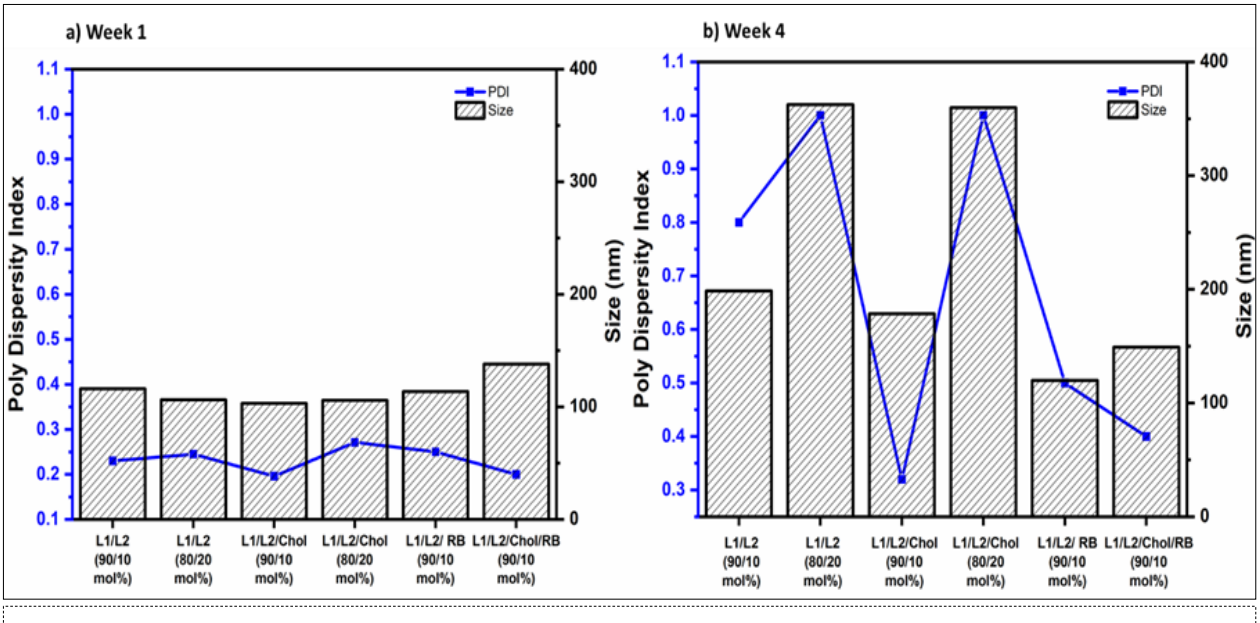

Figure 1. Size and PDI of the formulations for a) Week 1 b) Week 4

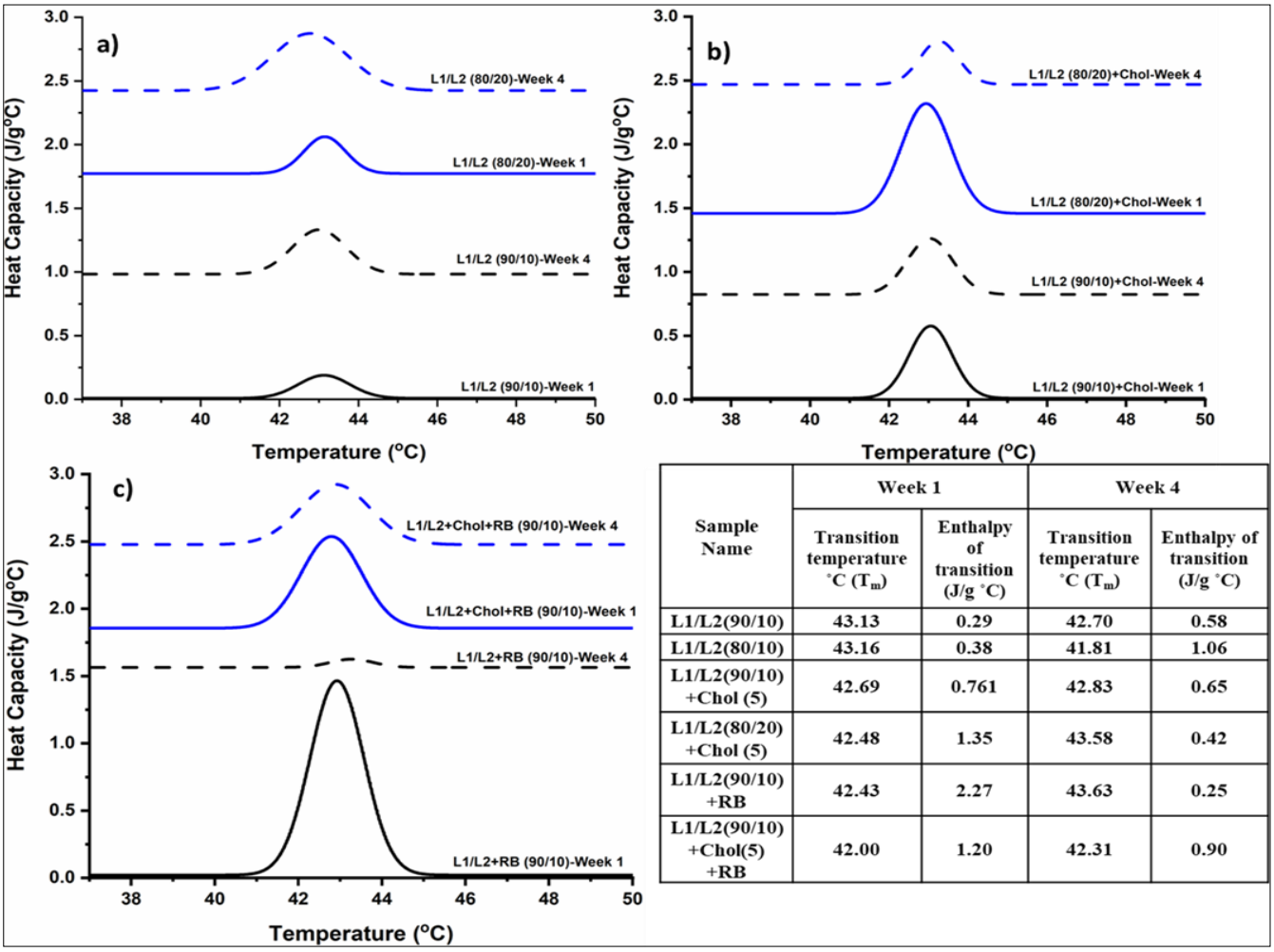

Sample Name	Week 1		Week 4	
	Transition temperature °C (T_m)	Enthalpy of transition (J/g °C)	Transition temperature °C (T_m)	Enthalpy of transition (J/g °C)
L1/L2(90/10)	43.13	0.29	42.70	0.58
L1/L2(80/10)	43.16	0.38	41.81	1.06
L1/L2(90/10) +Chol (5)	42.69	0.761	42.83	0.65
L1/L2(80/20) +Chol (5)	42.48	1.35	43.58	0.42
L1/L2(90/10) +RB	42.43	2.27	43.63	0.25
L1/L2(90/10) +Chol(5) +RB	42.00	1.20	42.31	0.90

Figure 2. DSC thermograms of liposomal formulations measured in weeks 1 and 4 a) DC8,9PC:DSPE- PEG-2000 (L1/L2) at (90/10) and (80/20) mole ratios b) L1/L2 (90/10) and (80/20) + 5 mol% cholesterol c) L1/L2 (90/10) only + 5 mol % cholesterol, encapsulated with riboflavin

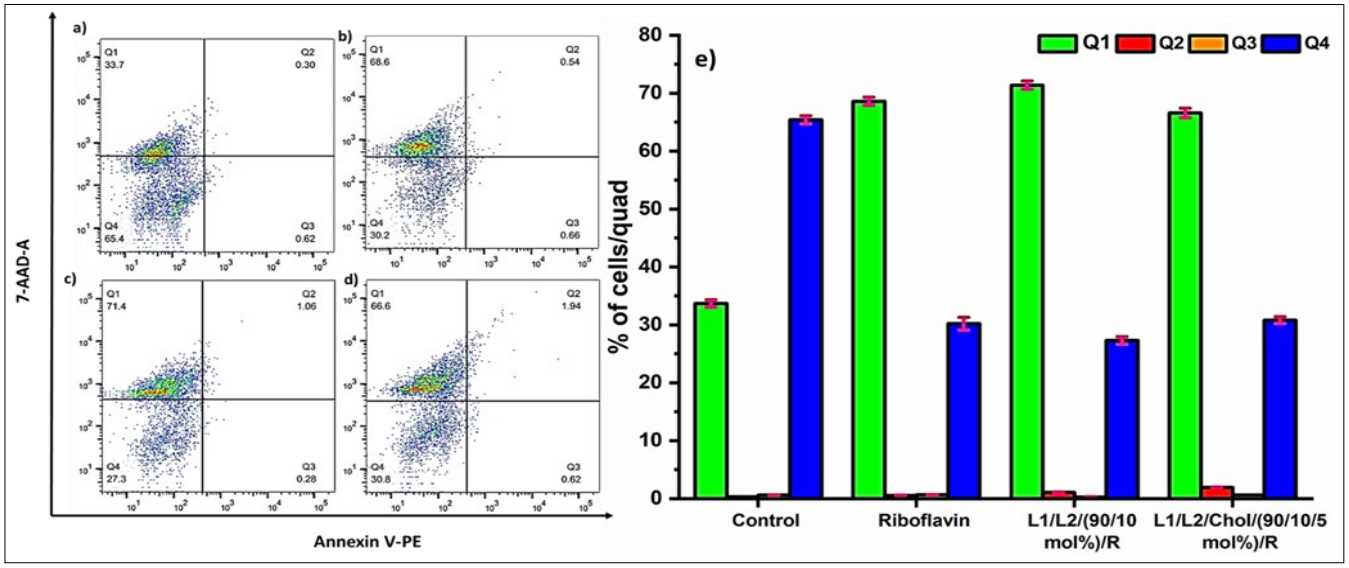

Figure 3. Apoptosis assay using Annexin V PE/7-AAD a) Control-Cells treated with UV b) Cells seeded with Unencapsulated Riboflavin and UV treated c) Cells seeded with Formulation L1/L2 (90/10 mol%)/RB and treated with UV d) Cells seeded with Formulation L1/L2/Chol (90/10/5 mol%)/RB and treated with UV e) Graphical representation of cell apoptosis in the four quadrants

The fluidity of the bilayer is more as we get closer to the transition temperatures of the liposomes. This is demonstrated by the change in enthalpy. The change in enthalpy (ΔH) is represented as follows [46],

$$\Delta H\,(Change\ in\ Enthalpy) = \Delta U\,(Change\ in\ Internal\ Energy) + \Delta(PV)\,(Change\ in\ Pressure\ x\ Volume) \quad \text{....(ii)}$$

The internal energy represents various molecular interactions occurring within the system. Since the liposomal formulations were sealed in T-zero hermetic pan during the DSC studies, the change in pressure (P) and volume (V) is considered negligible. Therefore, the change in enthalpy depends mostly on the inter-molecular interactions such as van der Waals forces occurring between the lipid, PEG and encapsulated riboflavin and intramolecular polar bonds.

The melting temperatures of pure $DC_{8,9}PC$, DSPE -PEG , and cholesterol are reported as 45°C, 52°C and 150°C respectively. [47–49]. Fig 3a) represents the thermograms of the formulations $DC_{8,9}PC$ liposomes containing 10 and 20 mol% of DSPE-PEG-2000 labelled as L1/L2 (90/10) and L1/L2 (80/20) by mol% respectively and measured at weeks 1 and 4. A slight decrease in the melting transition temperature of 0.43°C was observed for the formulation L1/L2 (90/10 mol%) over the four-week period. The associated enthalpy with the melting transition, which is also the indicator of the stability of the liposomal formulations was computed from the area under the melting peak and tabulated in Table 2. Despite the negligible shift in the melting temperature, the enthalpy of transition was found to be nearly doubled. With increased PEG from 10 to 20 mol% in the formulation L1/L2 (80/20 mol%), a significant shift towards a lower temperature from 43.16 °C to 41.81 °C denoted by blue lines on Fig 2a was observed. The temperature shift was accompanied a dramatic increase in the enthalpy by 178%. Adiscrepant observation in Fig 2b) thermograms was made in the presence cholesterol. 5 mol% of cholesterol was added to both L1/L2 at 90/10 and 80/20 formulations to study the effects of cholesterol on the stability of the formulations. L1/L2 (90/10) + 5 mol% cholesterol had imperceptible increase in transition temperature of 0.14°C and a decrease in enthalpy of 14.5% from week one to week four as observed in Fig 2b. However, L1/L2 (80/20) + 5 mol% showed a more prominent change in the temperature from 42. 48 °C to 43.58 °C and a significant decrease in enthalpy of 68.18% from week one to week 4. From Figs 2 a) and b), the L1/L2 (90/10) formulation demonstrated more consistent thermal behaviour with regards to change in enthalpy and melting temperature in the presence and absence of cholesterol observed in a period of four weeks. Fig 2c) compares the thermal stability of L1/L2 (90/10) formulations encapsulated with riboflavin in the presence and absence of cholesterol. A dramatic decrease in the enthalpy by 89% was noted by week 4 with L1/L2 (90/10) encapsulated formulations. However, the same formulations impregnated with 5 mol% cholesterol demonstrated a slight change in the enthalpy and melting temperature. DSC studies imply the role of cholesterol in acquiring thermal stability of the liposomal formulations.

Apoptotic Studies

Previous studies have extensively reported the toxicity of encapsulated riboflavin in cancerous cells[38, 50–52] and the non-toxic behaviour of the lipid formulations [48, 53]. This *in vitro* work further delved into investigating the nature of apoptosis of encapsulated riboflavin under UV radiation. The apoptosis was assessed using Annexin V PE and 7-AAD quadrants in DU145 cells as shown in Fig 3. Apoptosis is indicated by the increased intensity of Annexin V as it bind to the phosphatidylserine in the cancerous cells [54]. Q1 represents dead cells by necrosis (Annexin V PE-/7-AAD+),Q2 demonstrates dead cells by late apoptosis (Annexin V PE+/7-AAD+), Q3 represents early apoptosis (Annexin V PE+/7-AAD-) and Q4 represents live cells devoid of apoptosis or necrosis (Annexin V PE-/7-AAD-)[55].

Control UV treated cells (Fig 3a) were 65.4% viable. The addition of riboflavin and photoactivation resulted in increase in necrotic cells at 68.6% as seen in Figs 3b and e. Similarly, cells treated with photoactivated formulations L1/L2 (90/10 mol%) with encapsulated RB, and L1/L2 (90/10) + 5 mol% cholesterol with encapsulated RB showed an increase in necrotic cells by 71.4% and 66.6% respectively as depicted in Figs 3c-e. Riboflavin is known to produce reactive oxygen species (ROS) upon activation by UV radiation which are lethal to cancerous cells [35, 56]. The cancerous cell lines in the presence of unencapsulated riboflavin showed a maximum

necrotic rate of 68.6%. Riboflavin encapsulated photopolymerizable formulations, showed an equal to higher necrotic rate in the same cell lines. Our previous studies have shown that riboflavin encapsulated riboflavin formulations have >50% encapsulation efficiency [38]. This is noteworthy as encapsulated formulations shown similar rate of effectiveness as free riboflavin. The necrotic rate of cholesterol based formulation L1/L2 (90/10) with 5 mol% cholesterol was found to be lower than L1/L2 (90/10) alone, which probably attributes to the lower drug loading capacity by the liposomes in the presence of cholesterol. This could be due to the lower reduced fluidity caused by the cholesterol molecules in the lipid bilayer during the encapsulation process [57, 58]. This was also supported by our DSC studies that demonstrated insignificant change in melting behaviour of the liposomal formulations impregnated with cholesterol. It should also be noted that riboflavin in the absence of photoactivation does not induce apoptotic pathways and in fact, exhibits anti-proliferative/anti-migratory effects [55]. The mechanism of apoptosis/necrosis by ROS produced by encapsulated riboflavin is subject to further research.

Discussion

Physical Steric Stability

Agglomeration of liposomes is a key issue in drug delivery and vaccine design that can be addressed through electrostatic and steric stabilization shown schematically in Figs 4a and b. Another key requirement is their longer circulation times which can be achieved by rendering electrostatic stabilization that may be achieved by employing zwitterionic or uncharged surfaces to prevent their adherence to charged plasma proteins *in vivo* [59]. This work focused on using zwitterionic lipids to create liposome formulations, and to address the agglomeration issues, PEGylated lipids were incorporated. The incorporation of conjugated PEG or PEGylated lipids in liposomal formulations prevented the overall agglomeration as seen from the size measurements. PEG chains are grafted to the surface of the liposomes on one end and based on their concentration and density they result in mushroom or brush-type configuration as depicted in Fig 4.

At lower concentrations, the PEG chains do not interact with each other and assume a mushroom-like random coiled configuration shown in Fig 4c. With an increasing concentration, the mushroom regime transitions to brush regime in which the PEG chains begin to uncoil or branch out and interact with each other as shown in Fig 4d. The transition from mushroom to brush regime happens when the following condition is fulfilled [60].

$$X_p^{m\to b} > [\frac{A_1}{\pi a_m{}^2}] n_p^{-1.2} \quad \text{....(iii)}$$

Where $X_p{}^{m\to b}$ is the mole fraction of PEG; for PEG lipids with chains of molecular weights 2000 (n_p=45) is presumed to occur at 0.014.

A_1 is the membrane surface area per lipid molecule[60].

Brush regime is preferred for drug delivery application for steric stabilization and longer circulation time[61–63]. However, when the concentration of PEG chains in the brush regime increases the surrounding aqueous layer dehydrates resulting in aggregation[64]. This is observed in when the concentration of PEG lipids is increased from 10 to 20 mol% in LI/L2 (80/20 mol%) formulation, which aggregates after four weeks.

The hydrophilic nature of the elongated PEG chains in the brush regime tends to interact more with aqueous bulk than with the other grafted PEG chains of neighbouring liposomes, thereby preventing the agglomeration of the liposomes. The steric stabilization, $W(h)_{steric}$ between two liposomes of rendered PEG chains in brush regime of thickness Lb is quantified by

$$W(h)_{steric} = \frac{100RL_b^2}{\pi s^3} k_B T exp(\frac{-\pi h}{L_b}) \quad \text{....(iv)}$$

where *kB* is the Boltzmann constant, $Lb = (NEO \times l^{5/3} / s^{2/3})$. *NEO* is the number of monomers in the PEG chain, *l* is the effective segment length and *s* is the distance between the grafting points[65].

Thermal Stability

The presence of DSPE-PEG2000 at 10 mol% in L1/L2 (90/10) formulation enabled the steric stabilization of $DC_{8,9}PC$ vesicles as evidenced by the size and zeta potential measurements in Fig 1, which is further supported by previous studies [48].

The enthalpy of transitions which quantifies the inter and molecular interactions, was found to increase in L1/L2 (90/10) and L1/L2 (80/20) formulations from

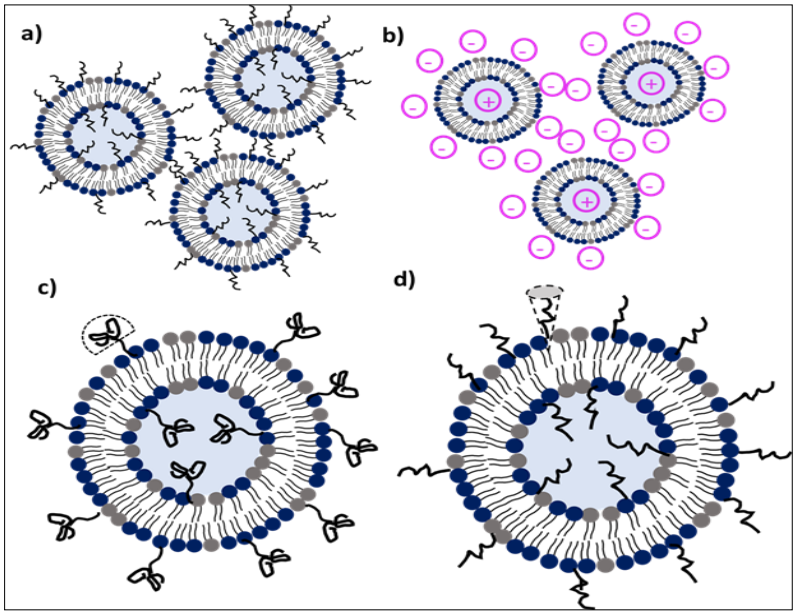

Figure 4. Schematic representation of a) steric stabilization of liposomes, b) electrostatic stabilization via opposite charges , c) mushroom regime with coiled PEG chains , and d) brush regime with extended PEG chains

week 1 to 4 with an accompanying decrease in the melting transition temperature as shown in Fig 2a. This is attributed primarily to the interaction and subsequent entangling of PEG chains which further increases the van der Waals forces. The energy required to overcome this van der Waals forces which is represented by an increase in enthalpy. Based on the DSC studies, it is noteworthy that increased concentration of PEGylated lipids from 10 to 20 mol% in the liposomal formulation, the resultant enthalpy of transition increases due to intermolecular interactions between the various lipid bilayer components.

Fig 2b) summarizes the combined effects of cholesterol and PEG on the thermal stability of the liposomal formulations. In L1/L2 (90/10) mol%, for every DSPE-PEG lipid there are 114 $DC_{8,9}PC$ lipid molecules. When 5 mol% cholesterol is added, there are 2 cholesterol molecules per one PEG molecule. It is implied that the addition of cholesterol to PEGylated lipids render thermal stability to the lipid bilayer owing to their known stabilizing properties of the liposomes. This is could possibly be due to the lowered molecular interactions between the lipid components in presence of cholesterol in the lipid bilayer. Cholesterol, being hydrophobic gets incorporated in the bilayer region of the liposomes that results in an reorganized packing and respacing of lipids in the bilayer[58, 66] limiting the interaction among the PEG chains which in turn lowers the van der Waals force [67]. This results in a slight increase in melting transition temperature is accompanied by a decrease in the enthalpy. Additionally, the presence of PEG and cholesterol also induce heterogenicity to the bilayer, resulting in a lateral phase separation[44, 68] which is supported by the broadening of melting peaks mostly seen during week 4 measurements indicated by blue lines on Fig. 2b.

DSC and size analysis indicated the stability of $DC_{8,9}PC$/DSPE-PEG2000 (90/10) with and without 5 mol% cholesterol, which were further encapsulated with riboflavin. The riboflavin encapsulated formulations in absence of cholesterol showed an enormous change in enthalpy suggesting major intermolecular events in the lipid bilayer as seen on Fig 2c. This is attributed to the hydrophilicity of riboflavin that results in their encapsulation in the aqueous core and bound on the hydrophilic headgroup region of the bilayer that further increases the spacing and packing between the lipids [38]. The presence of cholesterol, however, counterbalances this lipid disorganization due to riboflavin binding consequently reducing the molecular forces responsible for the enthalpy change. Additionally, it is proposed that the presence of riboflavin in the

aqueous core also prevents the entanglement of PEG chains in the formulation further reducing the interactions between the PEG groups thereby concurrently reducing the enthalpy change in encapsulated formulations.

Conclusion

The present study elucidated the distinct roles played by cholesterol and PEG in liposomal formulations by investigating varying concentration of each of the components in photo- polymerizable liposomes in the presence and absence of encapsulated riboflavin over a duration of four weeks. Following conclusions can be drawn based on the combined experimental and mechanistic studies:

PEG chains extend outward creating a layer around the liposomes that creates a steric layer that prevents liposomal agglomeration as supported by the lower polydispersity index, small hydrodynamic diameters, and surface charge measurements

Inclusion of cholesterol with PEGylated lipids at lower ratios lowers the overall enthalpy change arising from intermolecular interactions indicating the role of cholesterol in minimizing the molecular interactions and probably the bilayer fluidity

Encapsulated riboflavin further stabilized the formulations as confirmed by changes in the specific heat capacity and transition temperatures of the formulations

Acknowledgment

The presented work was conducted in the Interfacial Thermal and Transport laboratory at the University of Toledo and was supported by College of Engineering start-up grant.

Conflict of Interests

The authors declare no conflict of interest.

References

1. Torchilin, V. P., & Weissig, V. (2003). *Liposomes: a practical approach* (Vol. 264). Oxford University Press Oxford.
2. Çağdaş, M., Sezer, A. D., & Bucak, S. (2014). Liposomes as Potential Drug Carrier Systems for Drug Delivery. https://doi.org/10.5772/58459. In *Application of Nanotechnology in Drug Delivery*. InTech.
3. Vabbilisetty, P., & Sun, X. L. (2014). Liposome surface functionalization based on different anchoring lipids via Staudinger ligation. https://doi.org/10.1039/c3ob41721b. *Organic and Biomolecular Chemistry*, *12*(8), 1237–1244.
4. Riaz, M. K., Riaz, M. A., Zhang, X., Lin, C., Wong, K. H., et al. (2018, January 9). Surface functionalization and targeting strategies of liposomes in solid tumor therapy: A review. https://doi.org/10.3390/ijms19010195. *International Journal of Molecular Sciences*. MDPI AG.
5. Sun, C., Wang, J., Liu, J., Qiu, L., Zhang, W., et al. (2013). Liquid proliposomes of nimodipine drug delivery system: Preparation, characterization, and pharmacokinetics. https://doi.org/10.1208/s12249-013-9924-6. *AAPS PharmSciTech*, *14*(1), 332–338.
6. Alavi, M., Karimi, N., & Safaei, M. (2017, April 1). Application of various types of liposomes in drug delivery systems. https://doi.org/10.15171/apb.2017.002. *Advanced Pharmaceutical Bulletin*. Tabriz University of Medical Sciences.
7. Pattni, B. S., Chupin, V. V., & Torchilin, V. P. (2015). New Developments in Liposomal Drug Delivery. https://doi.org/10.1021/acs.chemrev.5b00046. *Chemical Reviews*. American Chemical Society.
8. Kumar Pramanik, S., Losada-Pérez, P., Reekmans, G., Carleer, R., D'Olieslaeger, M., et al. (2017). Physicochemical characterizations of functional hybrid liposomal nanocarriers formed using photo-sensitive lipids. https://doi.org/10.1038/srep46257. *Scientific Reports*, *7*(1), 46257.
9. S Barua, S. M. (2014). Challenges associated with penetration of nanoparticles across cell and tissue barriers: A review of current status and future prospects. *Nano Today*, *9*, 223–243.
10. RK Jain, T. S. (2010). Delivering nanomedicine to solid tumors. *Nat. Rev. Clin. Oncol.*, *7*, 653–664.
11. Maherani, B., Arab-Tehrany, E., R. Mozafari, M., Gaiani, C., & Linder, M. (2011). Liposomes: A Review of Manufacturing Techniques and Targeting Strategies. https://

doi.org/10.2174/157341311795542453. *Current Nanoscience*, *7*(3), 436–452.

12. Andresen, T. L., Jensen, S. S., & Jørgensen, K. (2005, January 1). Advanced strategies in liposomal cancer therapy: Problems and prospects of active and tumor specific drug release. https://doi.org/10.1016/j.plipres.2004.12.001. *Progress in Lipid Research*. Elsevier Ltd.
13. Raemdonck, K., Braeckmans, K., Demeester, J., & De Smedt, S. C. (2014). Merging the best of both worlds: hybrid lipid-enveloped matrix nanocomposites in drug delivery. https://doi.org/10.1039/C3CS60299K. *Chem. Soc. Rev.*, *43*(1), 444–472.
14. Yavlovich, A., Smith, B., Gupta, K., Blumenthal, R., & Puri, A. (2010). Light-sensitive lipid-based nanoparticles for drug delivery: design principles and future considerations for biological applications. https://doi.org/10.3109/09687688.2010.507788. *Molecular Membrane Biology*, *27*(7), 364–381.
15. Puri, A. (2013). Phototriggerable Liposomes: Current Research and Future Perspectives. https://doi.org/10.3390/pharmaceutics6010001. *Pharmaceutics*, *6*(1), 1–25.
16. Thet, N. T., Jamieson, W. D., Laabei, M., Mercer-Chalmers, J. D., & Jenkins, A. T. A. (2014). Photopolymerization of polydiacetylene in hybrid liposomes: Effect of polymerization on stability and response to pathogenic bacterial toxins. https://doi.org/10.1021/jp502586b. *Journal of Physical Chemistry B*, *118*(20), 5418– 5427.
17. Moon, J., Suh, H., Bershteyn, A., Stephan, M., materials, H. L.-N., et al. (n.d.). Interbilayer-crosslinked multilamellar vesicles as synthetic vaccines for potent humoral and cellular immune responses. *nature.com*. Retrieved from https://www.nature.com/articles/nmat2960
18. Jelinek, R., Systems, S. K.-C. C. S., & 2007, undefined. (2007). Biomolecular Sensing with Colorimetric Vesicles. https://doi.org/10.1007/128_2007_112. Springer, 277, 155– 180.
19. Lasic, D. D., & Needham, D. (1995). The "Stealth" Liposome: A Prototypical Biomaterial. https://doi.org/10.1021/cr00040a001. *Chemical Reviews*, *95*(8), 2601– 2628.
20. Napper, D. H. (1977). Steric stabilization. https://doi.org/10.1016/0021-9797(77)90150-3 *Journal of Colloid And Interface Science*, *58*(2), 390–407.
21. Stenkamp, V. S., & Berg, J. C. (1997). The role of long tails in steric stabilization and hydrodynamic layer thickness. https://doi.org/10.1021/la970173a. *Langmuir*, *13*(14), 3827–3832.
22. Selvamani, V. (2018). Stability Studies on Nanomaterials Used in Drugs. https://doi.org/10.1016/B978-0-12-814031-4.00015-5. In *Characterization and Biology of Nanomaterials for Drug Delivery: Nanoscience and Nanotechnology in Drug Delivery* (pp. 425–444). Elsevier.
23. Virden, J. W., & Berg, J. C. (1992). NaCl-induced Aggregation of Dipalmitoylphosphatidylglycerol Small Unilamellar Vesicles with Varying Amounts of Incorporated Cholesterol. https://doi.org/10.1021/la00042a007. *Langmuir*, *8*(6), 1532– 1537.
24. Demel, R., on, B. D. K.-B. et B. A. (BBA)-R., & 1976, undefined. (n.d.). The function of sterols in membranes. Elsevier. Retrieved from https://www.sciencedirect.com/science/article/pii/0304415776900083
25. Mohammed, A. R., Weston, N., Coombes, A. G. A., Fitzgerald, M., & Perrie, Y. (2004). Liposome formulation of poorly water soluble drugs: Optimisation of drug loading and ESEM analysis of stability. International Journal of Pharmaceutics, 285 (1–2), 23–34. https://doi.org/10.1016j.ijpharm.2004.07.010.
26. Liu, D. Z., Chen, W. Y., Tasi, L. M., & Yang, S. P. (2000). Microcalorimetric and shear studies on the effects of cholesterol on the physical stability of lipid vesicles. https://doi.org/10.1016/S0927-7757(00)00560-4. *Colloids and Surfaces A: Physicochemical and Engineering Aspects*, *172*(1–3), 57–67.
27. Bulbake, U., Doppalapudi, S., Kommineni, N., & Khan, W. (2017). Liposomal Formulations in Clinical Use: An Updated Review. Pharmaceutics, 9(4), 12. https://doi.org/10.3390/pharmaceutics9020012.
28. Rhodes, D. G., Blechner, S. L., Yager, P., & Schoen, P. E. (1988). Structure of polymerizable lipid

bilayers. I-1,2-bis(10,12-tricosadiynoyl)-sn-glycero-3 - phosphocholine, a tubule-forming phosphatidylcholine. https://doi.org/10.1016/0009-3084(88)90062-X. *Chemistry and Physics of Lipids*, *49*(1–2), 39–47.

29. Schnitzer, E., Pinchuk, I., Bor, A., Leikin-Frenkel, A., & Lichtenberg, D. (2007). Oxidation of liposomal cholesterol and its effect on phospholipid peroxidation. https://doi.org/10.1016/j.chemphyslip.2006.12.003. *Chemistry and Physics of Lipids*, *146*(1), 43–53.
30. Rudolphi-Skórska, E., Filek, M., & Zembala, M. (2017). The Effects of the Structure and Composition of the Hydrophobic Parts of Phosphatidylcholine-Containing Systems on Phosphatidylcholine Oxidation by Ozone. https://doi.org/10.1007/s00232-017-9976-8. *Journal of Membrane Biology*, *250*(5), 493–505.
31. Touitou, E., & Barry, B. (2006). *Enhancement in drug delivery*. Retrieved from https://www.taylorfrancis.com/books/9780429122316
32. Vejux, A., Malvitte, L., & Lizard, G. (2008). Side effects of oxysterols: Cytotoxicity, oxidation, inflammation, and phospholipidosis. https://doi.org/10.1590/S0100-879X2008000700001. *Brazilian Journal of Medical and Biological Research*. Associacao Brasileira de Divulgacao Cientifica.
33. Domínguez, R., Pateiro, M., Gagaoua, M., Barba, F. J., Zhang, W., et al. (2019, October 1). A comprehensive review on lipid oxidation in meat and meat products. https://doi.org/10.3390/antiox8100429. *Antioxidants*. MDPI AG.
34. Bharadwaz, V., & Maulick, V. (2015). Preparation and characterization of nanoparticles of carboxymethyl cellulose acetate butyrate containing acyclovir. https://doi.org/10.1007/s13204-015-0421-y.
35. Yang, M.-Y., Chang, C.-J., & Chen, L.-Y. (2017). Blue light induced reactive oxygen species from flavin mononucleotide and flavin adenine dinucleotide on lethality of HeLa cells. https://doi.org/10.1016/J.JPHOTOBIOL.2017.06.014. *Journal of Photochemistry and Photobiology B: Biology*, *173*, 325–332.
36. Kandzija, N., & Khutoryanskiy, V. V. (2017). Delivery of Riboflavin-5′- Monophosphate Into the Cornea: Can Liposomes Provide Any Enhancement Effects? https://doi.org/10.1016/j.xphs.2017.05.022. *Journal of Pharmaceutical Sciences*, *106*(10), 3041–3049.
37. Arboleda, A., Miller, D., Cabot, F., Taneja, M., Aguilar, M. C., et al. (2014). *Rose Bengal- and Riboflavin-mediated Photodynamic Therapy of Fungal Keratitis Isolates*. *Investigative Ophthalmology & Visual Science* (Vol. 55). [Association for Research in Vision and Ophthalmology, etc.]. Retrieved from https://iovs.arvojournals.org/article.aspx?articleid=2268222
38. Kalyanram, P., Gupta, A., & Stadler, I. (2019). Interaction of Riboflavin-5-Phosphate With Liposome Bilayers. https://doi.org/10.4018/jnn.2018010103. *Journal of Nanotoxicology and Nanomedicine*, *3*(1), 49–59.
39. Gupta, A., Mandal, D., Ahmadibeni, Y., Parang, K., & Bothun, G. (2011). Hydrophobicity drives the cellular uptake of short cationic peptide ligands. https://doi.org/10.1007/s00249-011-0685-4. *European Biophysics Journal*, *40*(6), 727– 736.
40. Ye, G., Gupta, A., DeLuca, R., Parang, K., & Bothun, G. D. (2010). Bilayer disruption and liposome restructuring by a homologous series of small Arg-rich synthetic peptides. https://doi.org/10.1016/j.colsurfb.2009.10.016. *Colloids and Surfaces B: Biointerfaces*, *76*(1), 76–81.
41. Gupta A, Gupta R, Kurwadkar, S. (2014). *Liposome encapsulated antimicrobial peptides: potential infectious diseases therapy: Handbook of Research on Diverse Applications of Nanotechnology in Biomedicine, Chemistry and Engineering.* IGI Global Publisher.
42. Kalyanram, P., Ma, H., Marshall, S., Goudreau, C., Cartaya, A., et al. (2020). Interaction of Amphiphilic Coumarin with DPPC/DPPS Lipid Bilayer: Effects of Concentration and Alkyl Tail Length. https://doi.org/10.1039/D0CP00696C. *Physical Chemistry Chemical Physics*.
43. Chiu, M., & Prenner, E. (2011). Differential scanning calorimetry: An invaluable tool for a detailed thermodynamic characterization of macromolecules and their interactions. https://doi.org/10.4103/0975-

7406.76463. In *Journal of Pharmacy and Bioallied Sciences* (Vol. 3, pp. 39–59). Wolters Kluwer - Medknow Publications.

44. Matsingou, C., & Demetzos, C. (2007). Calorimetric study on the induction of interdigitated phase in hydrated DPPC bilayers by bioactive labdanes and correlation to their liposome stability: The role of chemical structure. https://doi.org/10.1016/J.CHEMPHYSLIP.2006.10.004. *Chemistry and Physics of Lipids*, *145*(1), 45–62.
45. Cao, Z., Zhang, L., & Jiang, S. (2012). Superhydrophilic zwitterionic polymers stabilize liposomes. https://doi.org/10.1021/la302433a. *Langmuir*, *28*(31), 11625–11632.
46. Smith, J. M. (Joseph M., Van Ness, H. C. (Hendrick C. ., Abbott, M. M., & Swihart, M. T. (Mark T. (n.d.). *Introduction to chemical engineering thermodynamics*.
47. Abdulla, J. M. A., Tan, Y. T. F., & Darwis, Y. (2010). Rehydrated lyophilized rifampicin-loaded mPEG-DSPE formulations for nebulization. AAPS PharmSciTech, 11(2), 663–671.
48. https://doi.org/10.1208/s12249-010-9428-6. Viard, M., Reichard, H., Shapiro, B. A., Durrani, F. A., Marko, A. J., et al. (2018). Design and biological activity of novel stealth polymeric lipid nanoparticles for enhanced delivery of hydrophobic photodynamic therapy drugs. https://doi.org/10.1016/j.nano.2018.07.006. *Nanomedicine: Nanotechnology, Biology, and Medicine*, *14*(7), 2295–2305.
49. Rahman, S. A., Abdelmalak, N. S., Badawi, A., Elbayoumy, T., Sabry, N., et al. (2015). Formulation of tretinoin-loaded topical proniosomes for treatment of acne: In-vitro characterization, skin irritation test and comparative clinical study. https://doi.org/10.3109/10717544.2014.896428. *Drug Delivery*, *22*(6), 731–739.
50. Machado, D., Shishido, S. M., Queiroz, K. C. S., Oliveira, D. N., Faria, A. L. C., et al. (2013). Irradiated Riboflavin Diminishes the Aggressiveness of Melanoma In Vitro and In Vivo. https://doi.org/10.1371/journal.pone.0054269. *PLoS ONE*, *8*(1), e54269.
51. Bartmann, L., Schumacher, D., Von Stillfried, S., Sternkopf, M., Alampour-Rajabi, S., et al. (2019). Evaluation of riboflavin transporters as targets for drug delivery and theranostics. https://doi.org/10.3389/fphar.2019.00079. *Frontiers in Pharmacology*, *10*(FEB), 79.
52. Ozsvari, B., Bonuccelli, G., Sanchez-Alvarez, R., Foster, R., Sotgia, F., et al. (2017). Targeting flavin-containing enzymes eliminates cancer stem cells (CSCs), by inhibiting mitochondrial respiration: Vitamin B2 (Riboflavin) in cancer therapy. https://doi.org/10.18632/aging.101351. *Aging*, *9*(12), 2610–2628.
53. Yavlovich, A., Singh, A., Blumenthal, R., & Puri, A. (2011). A novel class of photo- triggerable liposomes containing DPPC:DC $_{8,9}$PC as vehicles for delivery of doxorubcin to cells. https://doi.org/10.1016/j.bbamem.2010.07.030. *Biochimica et Biophysica Acta - Biomembranes*, *1808*(1), 117–126.
54. Amawi, H., Karthikeyan, C., Pathak, R., Hussein, N., Christman, R., et al. (2017). Thienopyrimidine derivatives exert their anticancer efficacy via apoptosis induction, oxidative stress and mitotic catastrophe. https://doi.org/10.1016/j.ejmech.2017.07.028. *European Journal of Medicinal Chemistry*, *138*, 1053–1065.
55. Mikkelsen, K., Prakash, M. D., Kuol, N., Nurgali, K., Stojanovska, L., et al. (2019). Anti-tumor effects of vitamin B2, B6 and B9 in promonocytic lymphoma cells. https://doi.org/10.3390/ijms20153763. *International Journal of Molecular Sciences*, *20*(15).
56. Dolmans, D. E. J. G. J., Fukumura, D., & Jain, R. K. (2003). Photodynamic therapy for cancer. https://doi.org/10.1038/nrc1071. *Nature Reviews Cancer*, *3*(5), 380–387.
57. Mohammed, A. R., Weston, N., Coombes, A. G. A., Fitzgerald, M., & Perrie, Y. (2004). Liposome formulation of poorly water soluble drugs: Optimisation of drug loading and ESEM analysis of stability. https://doi.org/10.1016/j.ijpharm.2004.07.010. *International Journal of Pharmaceutics*, *285*(1–2), 23–34.
58. Briuglia, M. L., Rotella, C., McFarlane, A., & Lamprou, D. A. (2015). Influence of cholesterol on liposome stability and on in vitro drug release. https://doi.org/10.1007/s13346-015-0220-8. *Drug*

Delivery and Translational Research, *5*(3), 231–242.

59. Owens, D. E., & Peppas, N. A. (2006, January 3). Opsonization, biodistribution, and pharmacokinetics of polymeric nanoparticles. https://doi.org/10.1016/j.ijpharm.2005.10.010. International Journal of Pharmaceutics. Elsevier.
60. Marsh, D., Bartucci, R., & Sportelli, L. (2003, September 2). Lipid membranes with grafted polymers: Physicochemical aspects. https://doi.org/10.1016/S0005-2736(03)00197-4. *Biochimica et Biophysica Acta - Biomembranes*. Elsevier.
61. Li, S., the, L. H.-J. of controlled release: official journal of, & 2010, undefined. (n.d.). Stealth nanoparticles: high density but sheddable PEG is a key for tumor targeting. ncbi.nlm.nih.gov. Retrieved from https://www.ncbi.nlm.nih.gov/pmc/articles/PMC2902652/
62. Yang, Q., Jones, S. W., Parker, C. L., Zamboni, W. C., Bear, J. E., et al. (2014). Evading immune cell uptake and clearance requires PEG grafting at densities substantially exceeding the minimum for brush conformation. https://doi.org/10.1021/mp400703d. *Molecular Pharmaceutics*, *11*(4), 1250–1258.
63. Salmaso, S., & Caliceti, P. (n.d.). Stealth Properties to Improve Therapeutic Efficacy of Drug Nanocarriers. https://doi.org/10.1155/2013/374252. *Journal of Drug Delivery*, *2013*.
64. Shen, Z., Ye, H., Kröger, M., & Li, Y. (2018). Aggregation of polyethylene glycol polymers suppresses receptor-mediated endocytosis of PEGylated liposomes. https://doi.org/10.1039/c7nr09011k. *Nanoscale*, *10*(9), 4545–4560.
65. Johnsson, M. (2001). *Comprehensive Summaries of Uppsala Dissertations from the Faculty of Science and Technology 629 Sterically Stabilised Liposomes and Related Lipid Aggregates Fundamental Studies on Aggragate Structure and Stability*. Retrieved from http://www.diva-portal.org/smash/record.jsf?pid=diva2:167878
66. Lee, S. C., Lee, K. E., Kim, J. J., & Lim, S. H. (2005). The effect of cholesterol in the liposome bilayer on the stabilization of incorporated retinol. https://doi.org/10.1080/08982100500364131. *Journal of Liposome Research*, *15*(3–4), 157–166.
67. Bedu-Addo, F. K., Tang, P., Xu, Y., & Huang, L. (1996). Effects of polyethyleneglycol chain length and phospholipid acyl chain composition on the interaction of polyethyleneglycol-phospholipid conjugates with phospholipid: implications in liposomal drug delivery. https://doi.org/10.1023/a:1016091314940. *Pharmaceutical research*, *13*(5), 710–7.
68. Hashizaki, K., Taguchi, H., Itoh, C., Sakai, H., Abe, M., et al. (2003). Effects of poly(ethylene glycol) (PEG) chain length of PEG-lipid on the permeability of liposomal bilayer membranes. https://doi.org/10.1248/cpb.51.815. *Chemical and Pharmaceutical Bulletin*, *51*(7), 815–820.